Therapeutics

FORUM ORIGINAL RESEARCH COMMUNICATION

Oligonol Inhibits Dextran Sulfate Sodium-Induced Colitis and Colonic Adenoma Formation in Mice

Hye-Won Yum,[1] Xiancai Zhong,[1] Jin Park,[1] Hye-Kyung Na,[2] Nayoung Kim,[3] Hye Seung Lee,[4] and Young-Joon Surh[1]

Abstract

Aims: To evaluate the effects of oligonol administration on experimentally induced colitis and colonic adenoma formation. *Results:* Oral administration of oligonol protected against mouse colitis induced by dextran sulfate sodium (DSS). Under the same experimental conditions, oligonol administration significantly inhibited the activation of nuclear factor-kappa B and signal transducer and activator of transcription (STAT) 3 and expression of cyclooxygenase-2 (COX-2), inducible nitric oxide synthase (iNOS), and cyclin D1 in the mouse colon. Further, oligonol inhibited azoxymethane-initiated and DSS-promoted adenoma formation in the mouse colon. Oligonol administration also attenuated lipid peroxidation (malondialdehyde) and protein oxidation (4-hydroxy-2-nonenal), thereby preventing oxidative stress-induced apoptosis of colonic epithelial cells. *In vitro* studies demonstrated that oligonol treatment reduced lipopolysaccharide-induced expression of *interleukin (IL)-1β, tumor necrosis factor α, il-6, cox-2,* and *inos* in murine macrophage RAW 264.7 cells. In another study, oligonol upregulated the antioxidant gene expression in the intestinal epithelial CCD841CoN cells and in the mouse colon. *Innovation:* Oligonol, an innovative formulation of catechin-type oligomers derived from the lychee fruit extract, was tested in this study for the first time to evaluate its effects on experimentally induced colitis and colonic adenoma formation in mice. *Conclusion:* Oligonol is effective in protecting against DSS-induced mouse colitis and colon carcinogenesis, suggesting that this polyphenol formulation may have a potential for the amelioration of inflammatory bowel disease and related disorders. *Antioxid. Redox Signal.* 19, 102–114.

Introduction

THE INFLAMMATORY BOWEL DISEASE (IBD), such as ulcerative colitis and Crohn's disease, is a chronic relapsing disease of the intestine. In IBD, the immune response is initiated by the interaction among the components of the innate immune system, including macrophages, dendritic cells, and antigens (22). In addition, the intestinal epithelium is also actively involved in the maintenance of immune homeostasis in the gut (1).

Bacterial products such as lipopolysaccharides (LPS) are recognized by mucosal macrophages *via* Toll-like receptor (TLR) 4. It is accompanied by an increased capacity of these cells to produce interleukin (IL)-1β, tumor necrosis factor

Innovation

A majority of naturally occurring polyphenols exist in a polymeric form and hence have a poor bioavailability when intaken by humans as a part of the diet. Oligonol is the low-molecular-weight oligomeric polyphenol, which is produced by an innovative manufacturing process. Since oligonol mainly consists of oligomers, it is anticipated to be absorbed from the gut to a greater extent than the general polyphenol extracts. We speculate that ingested oligonol could reach the colon more readily than the polymer and protects against colitis by acting directly on the intestinal epithelial cells.

[1]Tumor Microenvironment Global Core Research Center, College of Pharmacy, Seoul National University, Seoul, South Korea.
[2]Department of Food and Nutrition, College of Human Ecology, Sungshin Women's University, Seoul, South Korea.
Departments of [3]Internal Medicine and [4]Pathology, Seoul National University Bundang Hospital, Seongnam, Gyeonggi-do, South Korea.

(TNF) α, and IL-6, causing the stimulation of nuclear factor-kappa B (NF-κB) and signal transducer and activator of transcription (STAT) 3 activation (20).

Five members of the NF-κB subunits include p65 (RelA), RelB, c-Rel, p50/p105 (NF-κB1), and p52/p100 (NF-κB2). In the canonical pathway, the p65/p50 heterodimer remains inactive under the physiological condition by forming a complex with the inhibitor of κB (IκB), but becomes activated in response to diverse proinflammatory stimuli through increased phosphorylation and degradation of IκBα by the ubiquitin–proteasome system, thereby releasing the functionally active NF-κB (9) and regulating the transcription of genes encoding cyclooxygenase-2 (COX-2) and inducible nitric oxide synthase (iNOS) (12).

Activation of STAT3 is dependent on phosphorylation of tyrosine residue 705 in the C-terminal transactivation domain (TAD), which facilitates the dimerization of STAT3. The activated dimer then translocates into the nucleus and upregulates the genes encoding apoptosis inhibitors (e.g., Bcl-x1 and Mcl-1) and cell cycle regulators (e.g., cyclins D1/D2 and c-Myc) (2).

To cope with noxious insults, our body is endowed with efficient defense systems that detoxify and eliminate those harmful chemicals and their metabolites. Expression of cytoprotective enzymes and related proteins, including heme oxygenase-1 (HO-1), NAD(P)H:quinone oxidoreductase 1 (NQO-1), thioredoxin (TXN), and glutathione peroxidase 2 (GPx-2), is believed to be an important means of protecting cells against oxidative stress and other toxic insults. Free radical-mediated damage is exacerbated by the depletion of these above enzymatic antioxidant defenses accompanying the inflammatory process (3).

Colorectal cancer is one of the most serious complications of IBD. Dextran sulfate sodium (DSS) is toxic to colonic epithelium, inducing severe colitis, which mimics human IBD (5). DSS-induced generation of reactive oxygen species (ROS) is responsible for inflammatory as well as oxidative tissue damage (19). It has been demonstrated that treatment with DSS in combination with the carcinogen azoxymethane (AOM) enhances the development of aberrant crypt foci in rats (25) and adenocarcinoma in mice (24).

A wide variety of phenolic substances derived from edible plants have been reported to retain marked antioxidative and anti-inflammatory properties (6). Dietary polyphenols attenuate colonic signs of inflammation and autoimmunity (23). Oligonol, a standardized formulation consisting of 17.6% of catechin-type monomers and 18.6% of proanthocyanidin dimers and trimers derived from grape seeds or lychee fruit, possesses antioxidative and anti-inflammatory properties. Oligonol inhibited glucose-induced NF-κB activation in cultured renal tubular epithelial cells (8). In addition, oligonol induced apoptosis in the human breast cancer cells through modulation of the proapoptotic Bcl-2 family proteins and the mitogen-activated protein (MAP) kinase kinase (MEK)/extracellular signal-regulated protein kinase (ERK) signaling pathways (11). Topically applied oligonol inhibited the activation of kinases, the DNA binding of CCAAT/enhancer-binding protein (C/EBP) and activator protein-1 (AP-1), and subsequent expression of COX-2 in mouse skin irradiated with ultraviolet B (16). In addition, oligonol inhibited 12-O-tetradecanoylphorbol-13-acetate (TPA)-induced COX-2

expression by blocking the activation of NF-κB and C/EBP, as well as MAP kinases, and suppressed chemically induced mouse skin tumorigenesis (17).

As a part of the program evaluating the health beneficial effects of oligonol, we examined the effects of oligonol on the development of colonic inflammation induced by DSS in Crl:CD1 (ICR) mice. Further, the effect of oligonol on AOM plus DSS-induced colonic adenoma formation was also assessed in these mice.

Results

Oligonol ameliorated pathological symptoms in a mouse DSS-induced colitis model

The body weight of DSS-treated mice was significantly decreased after the day 4. However, oral administration of oligonol attenuated the body weight loss during the DSS treatment (Fig. 1A). Based on the severity of stool consistency and rectal bleeding, DSS-induced pathogenic conditions were scored from 0 to 4 (18). The sum was given into a form of the disease activity index (DAI). Mice treated with DSS exhibited serious symptoms with liquid stool and large amount of rectal bleeding. Oligonol administration ameliorated the severity of diarrhea and rectal bleeding (Fig. 1B). In addition, mice given DSS developed colitis as evidenced by thickening of the bowel wall and shortening of the colorectal length. Oral administration of oligonol dampened DSS-induced shortening of the colorectal length (Fig. 1C). We also performed histological evaluation of dysplasia in the colonic crypts using hematoxylin and eosin (H&E) staining. While exposure to DSS completely disrupted the architecture of colonic mucosa and induced infiltration of inflammatory cells and expansion of lamina propria, mice given oligonol exhibited a preserved colonic structure, clearance of inflammatory cells, and prevention of lamina propria expansion (Fig. 1D, E).

Oligonol attenuated DSS-induced oxidative stress and apoptosis in mouse colonic mucosa

Increased ROS production caused by DSS has been reported to induce oxidative injury in colonic mucosa (19). DSS administration increased the levels of malondialdehyde (MDA) and 4-hydroxy-2-nonenal (4-HNE), two major hallmarks of ROS-induced oxidative stress, in the mouse colon, and this was attenuated by oligonol administration (Fig. 2A, B, respectively). Oxidative stress can also cause apoptosis. Oligonol also decreased DSS-induced intestinal epithelial cell apoptosis detected by the terminal deoxynucleotidyl transferase dUTP nick-end labeling (TUNEL) assay (Fig. 2C).

Oligonol inhibited DSS-induced activation of NF-κB and STAT3 and their target protein expression in mouse colon

NF-κB and STAT3 are representative redox-sensitive transcription factors that play key roles in intracellular inflammatory signal transduction. Activation of NF-κB is dependent on its release from IκBα, which requires phosphorylation of the latter protein. Oligonol attenuated the DSS-induced phosphorylation and subsequent degradation of IκBα (Fig. 3A). Phosphorylation of p65 at the Ser^{536} residue located in the TAD of NF-κB is also important for activation of this transcription factor (21). Oligonol inhibited the DSS-induced
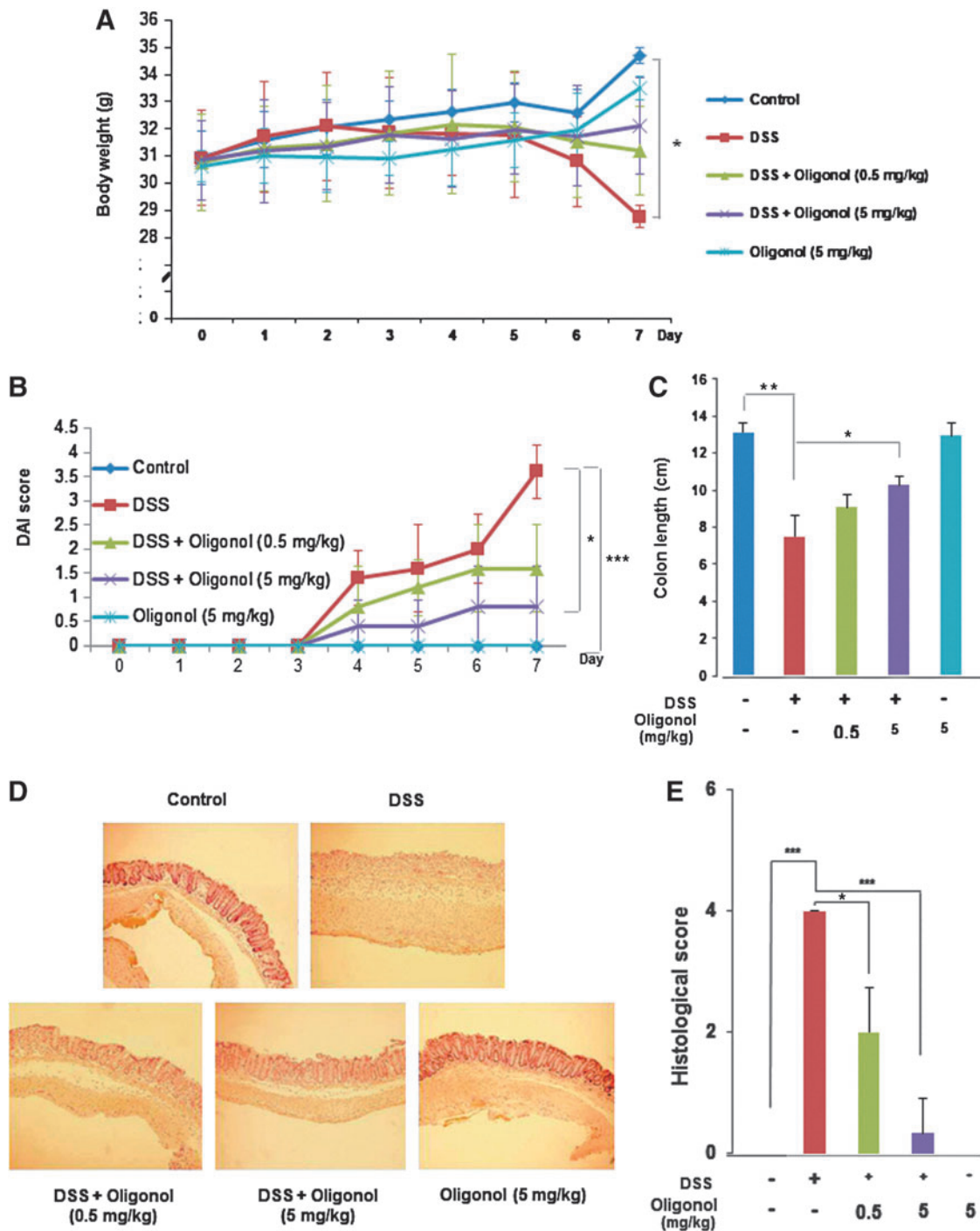
FIG. 1. Oligonol ameliorated pathological symptoms in a mouse DSS-induced colitis model. Male ICR mice (5 weeks of age) were treated with 3% DSS in drinking water for 7 days. Oligonol (0.5 or 5 mg/kg/day) was mixed in tap water and given orally for 7 days before DSS treatment and 7 days together with 3% DSS. **(A)** Gradual changes of body weight during DSS administration in mice. **(B)** Disease activity index (DAI) as the sum of stool consistency and rectal bleeding was scored from 0 to 4. **(C)** The comparison of the colon length at the day 7. **(D)** Representative distal colon sections stained with hematoxylin and eosin (H&E). Magnifications×100. **(E)** Histologic inflammatory score. Results are expressed as means±SD ($n = 5$, in each group). $*p < 0.05$, $**p < 0.01$ and $***p < 0.001$. DSS, dextran sulfate sodium; SD, standard deviation.

phosphorylation and nuclear translocation of p65, the major functionally active subunit of NF-κB (Fig. 3A). It also abolished the DSS-induced expression of COX-2 and iNOS in the mouse colon, two major proinflammatory enzymes whose expression is mainly regulated by NF-κB (Fig. 4A). Likewise,

STAT3 is mainly activated *via* IL-6-gp130-JAK signaling, leading to a direct phosphorylation on Tyr[705]. Oligonol exerted a significant inhibitory effect on DSS-induced phosphorylation of STAT3 at Tyr[705] (Fig. 3B) and expression of its target protein cyclin D1 (Fig. 4B).
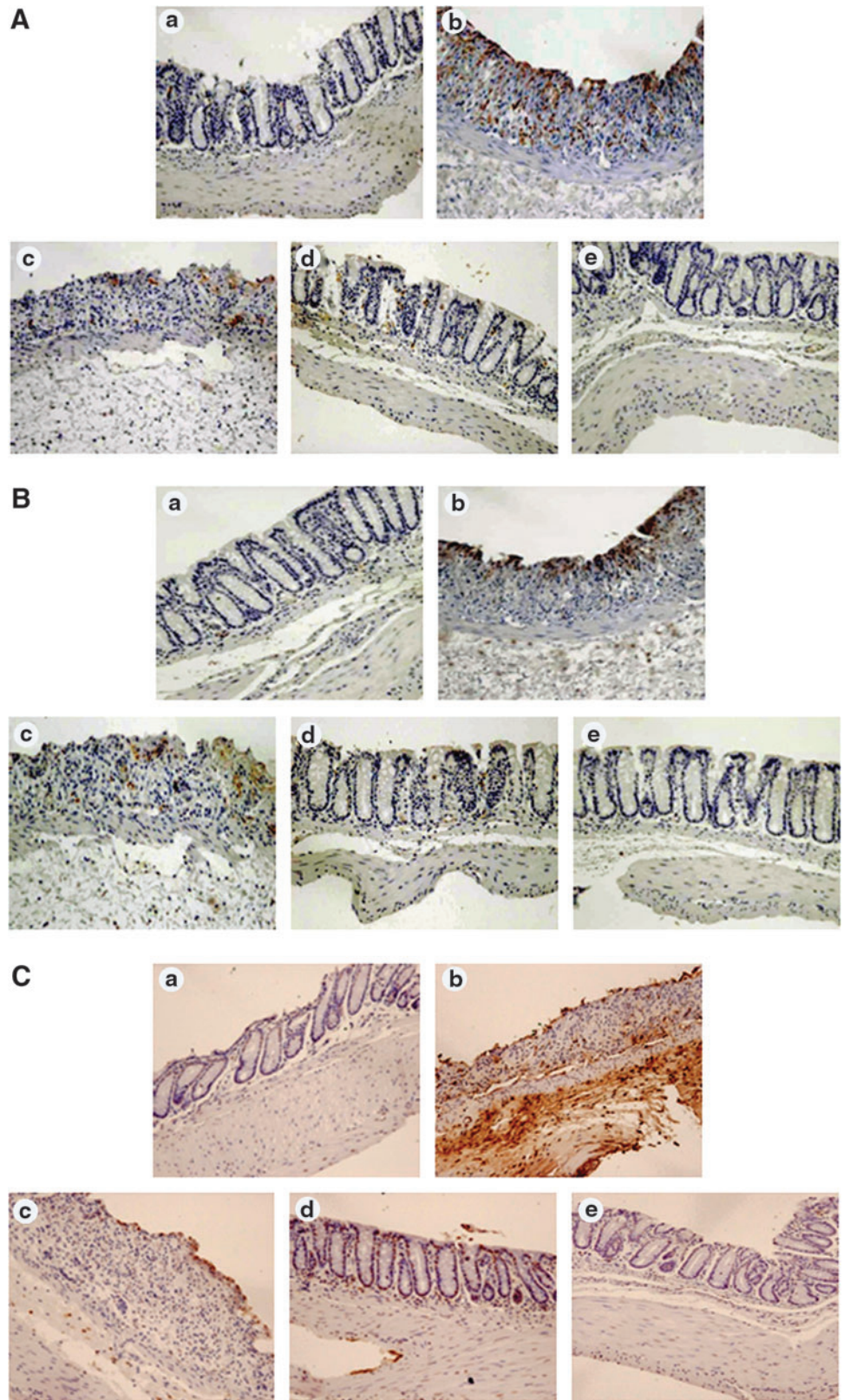
FIG. 2. Oligonol attenuated DSS-induced oxidative stress and apoptosis in mouse colon. Immunohistochemical detection of MDA **(A)** and 4-HNE-modified protein (brown spots) **(B)** in mouse colon. Magnifications×200. **(C)** A representative photomicrograph showing apoptotic cells stained with the ApopTag® Kits to detect DNA strand breaks. The experimental details are described in the Materials and Methods section. Magnifications×200. **(a)** Control; **(b)** DSS alone; **(c)** DSS + Oligonol (0.5 mg/kg); **(d)** DSS + Oligonol (5 mg/kg); **(e)** Oligonol (5 mg/kg) alone. Animal treatment and other experimental conditions are described in the Materials and Methods section.

Oligonol administration also ameliorated pathological symptoms in the trinitrobenzene sulfonic acid (TNBS)-induced mouse colitis model (Supplementary Fig. S1). Likewise, TNBS-induced p65 phosphorylation and the expression of COX-2 and iNOS were inhibited by oligonol (Supplementary Fig. S2). We also attempted to evaluate the anti-inflammatory effects of oligonol in IL-10 knockout (KO) mouse model. However, no significant colitis was developed spontaneously in these mice (Supplementary Fig. S3).
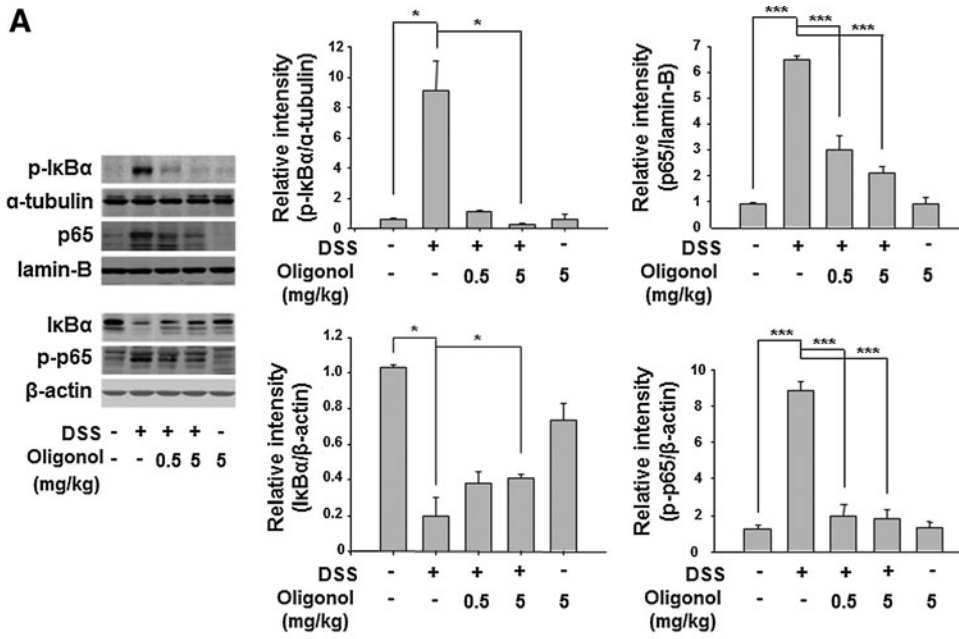
A

B

FIG. 3. **Oligonol inhibited DSS-induced activation of NF-κB and STAT3 in mouse colon. (A)** p-IκBα (Ser32/36), IκBα, p65, and p-p65 (Ser536), and **(B)** p-STAT3 (Tyr705) levels in the supernatants of colon strips of control mice, DSS-treated mice, oligonol (0.5 mg/kg)+DSS-treated mice, oligonol (5 mg/kg)+DSS-treated mice, and oligonol-treated mice (n=5, in each group). Data are expressed as means±SE. *p < 0.05, **p < 0.01, and ***p < 0.001. IκB, inhibitor of κB; NF-κB, nuclear factor-kappa B; STAT3, signal transducer and activator of transcription 3; SE, standard error.
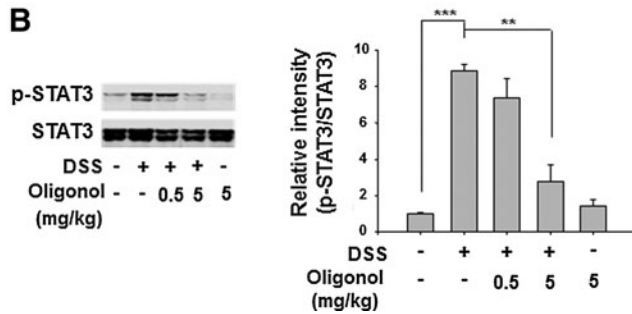
Oligonol inhibited LPS-induced proinflammatory gene expression in RAW 246.7 cells

After evaluation of anti-inflammatory activity of oligonol in the DSS-induced mouse colitis model, we examined its effect on expression of cytokines in macrophages upon stimulation with LPS, which is one of the most potent proinflammatory agonists for monocytes and macrophages. Oligonol treatment inhibited LPS-induced expression of *il-1β*, *tnf-α*, *il-6*, *cox-2*, and *inos* at
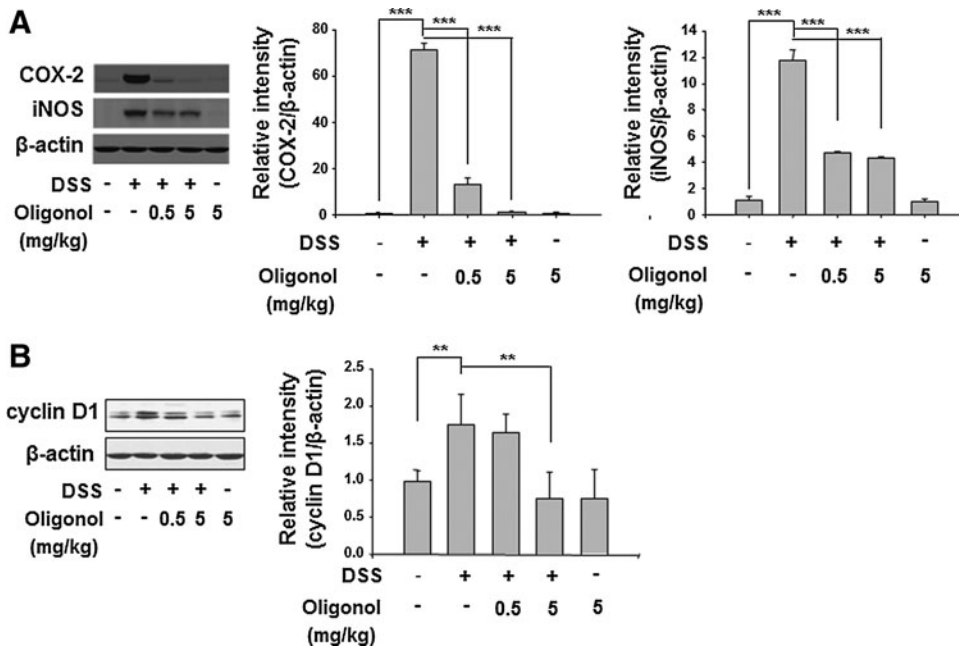
A

B

FIG. 4. **Oligonol inhibited DSS-induced expression of COX-2, iNOS, and cyclin D1 in mouse colon. (A)** COX-2 and iNOS and **(B)** cyclin D1 levels in the supernatants of colon strips of control mice, DSS-treated mice, oligonol (0.5 mg/kg)+DSS-treated mice, oligonol (5 mg/kg)+DSS-treated mice, and oligonol-treated mice (n=5 each group). Data are expressed as means±SE. **p < 0.01 and ***p < 0.001. COX-2, cyclooxygenase-2; iNOS, inducible nitric oxide synthase.

FIG. 5. Oligonol induced LPS-induced proinflammtory gene expression in RAW 246.7 cells. Reverse transcription–polymerase chain reaction (RT-PCR) analysis of LPS-induced mRNA expression of cytokines, *cox-2*, and *inos* in RAW 246.7 cells. Data represent three independent experiments ($n=3$). Results are expressed as means±SE. $*p<0.05$, $**p<0.01$, and $***p<0.001$. LPS, lipopolysaccharide.
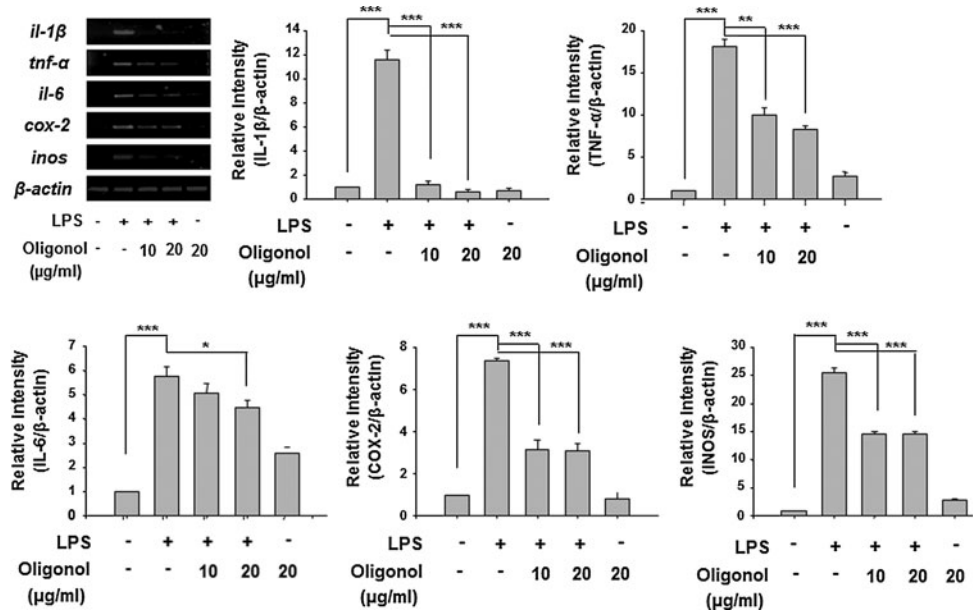

FIG. 6. Oligonol induced the expression of antioxidant enzymes in CCD841CoN cells for the indicated durations. (A) RT-PCR analysis of mRNA expression of *HO-1*, *NQO-1*, *MnSOD*, and *TRX* in CCD841CoN cells. **(B)** Western blot analysis of HO-1, NQO-1, and TXNRD1 protein expression in CCD841CoN cells. Data represent three independent experiments ($n=3$). Results are expressed as means±SE. $*p<0.05$, $**p<0.01$, and $***p<0.001$. HO-1, heme oxygenase-1; MnSOD, manganese superoxide dismutase; NQO-1, NAD(P)H:quinone oxidoreductase 1; TXNRD1, thioredoxin reductase 1.

107
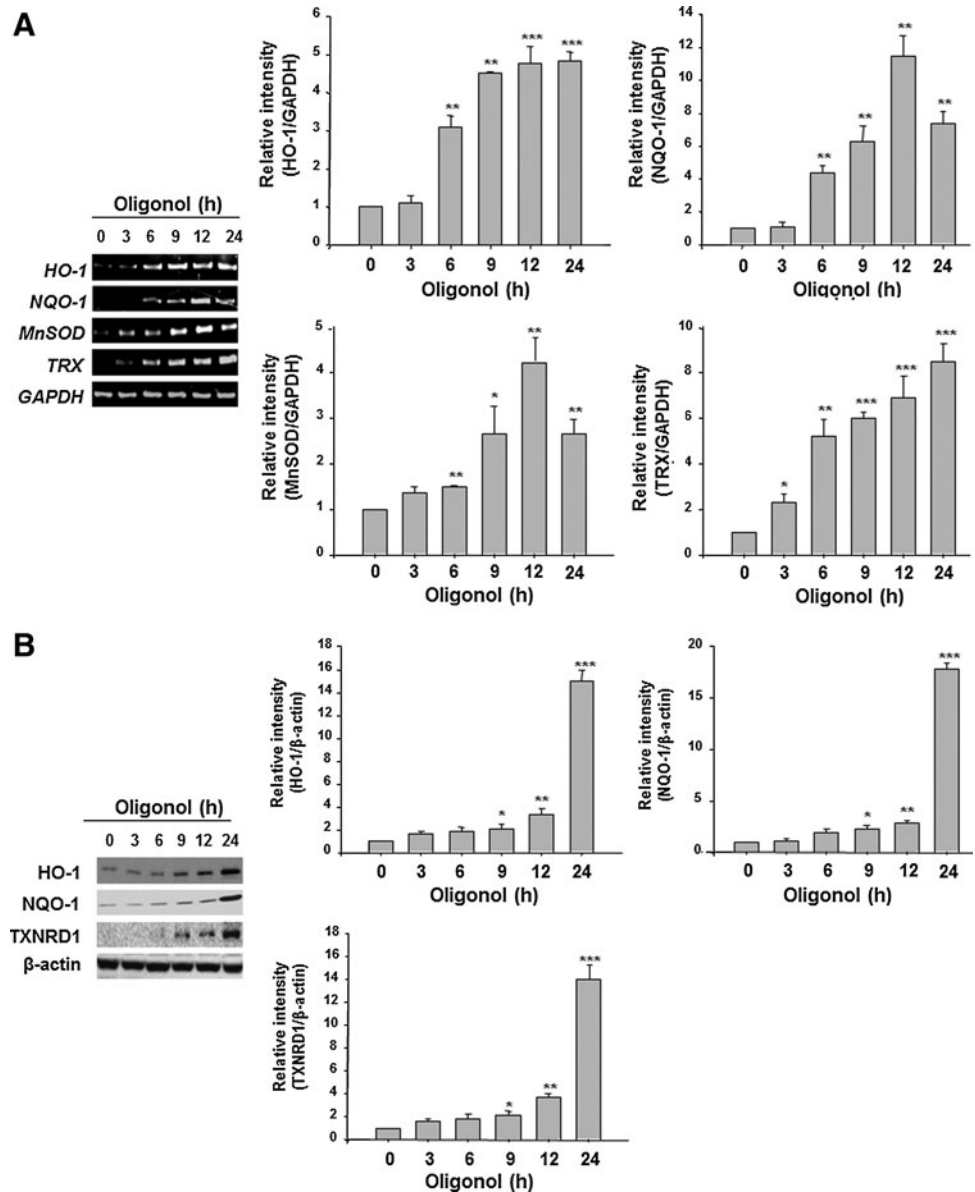
the mRNA level in mouse macrophage RAW 264.7 cells (Fig. 5). These data suggest that oligonol may regulate the macrophage functions in DSS-induced mouse colitis, thereby decreasing proinflammatory cytokine production.

Oligonol induced the expression of antioxidant enzymes in CCD841CoN cells and in the mouse colon

Since NF-κB or STAT3 are redox sensitive and their activation is mediated by ROS to some extent, we investigated whether oligonol could potentiate the antioxidative capacity of intestinal epithelial cells in the context of its inactivation of aforementioned transcription factors in mouse colon. Oligonol at a concentration at 10 μg/ml or 20 μg/ml had no effect on the viability of both RAW 246.7 cells and CCD841CoN cells (Supplementary Fig. S4). Oligonol treatment increased mRNA expression of

HO-1, NQO-1, manganese superoxide dismutase (MnSOD), and TRX in CCD841CoN cells (Figs. 6A and 7A). The protein levels of HO-1, NQO-1, and thioredoxin reductase 1 (TXNRD1) were also elevated by oligonol treatment (Figs. 6B and 7B). As demonstrated in Figure 8, oligonol administration upregulated the expression levels of HO-1, NQO-1, TRX 1, and GPx-2 in the mouse colon in vivo.

Oligonol inhibited AOM plus DSS-induced mouse colon carcinogenesis

Inflammation can promote the carcinogenesis as seen in IBD-associated CRC. Oligonol has an inhibitory effect on DSS-induced mouse colitis, which mimics the human IBD. This prompted us to determine whether oligonol could also inhibit colon tumor formation by employing an AOM-initiated and
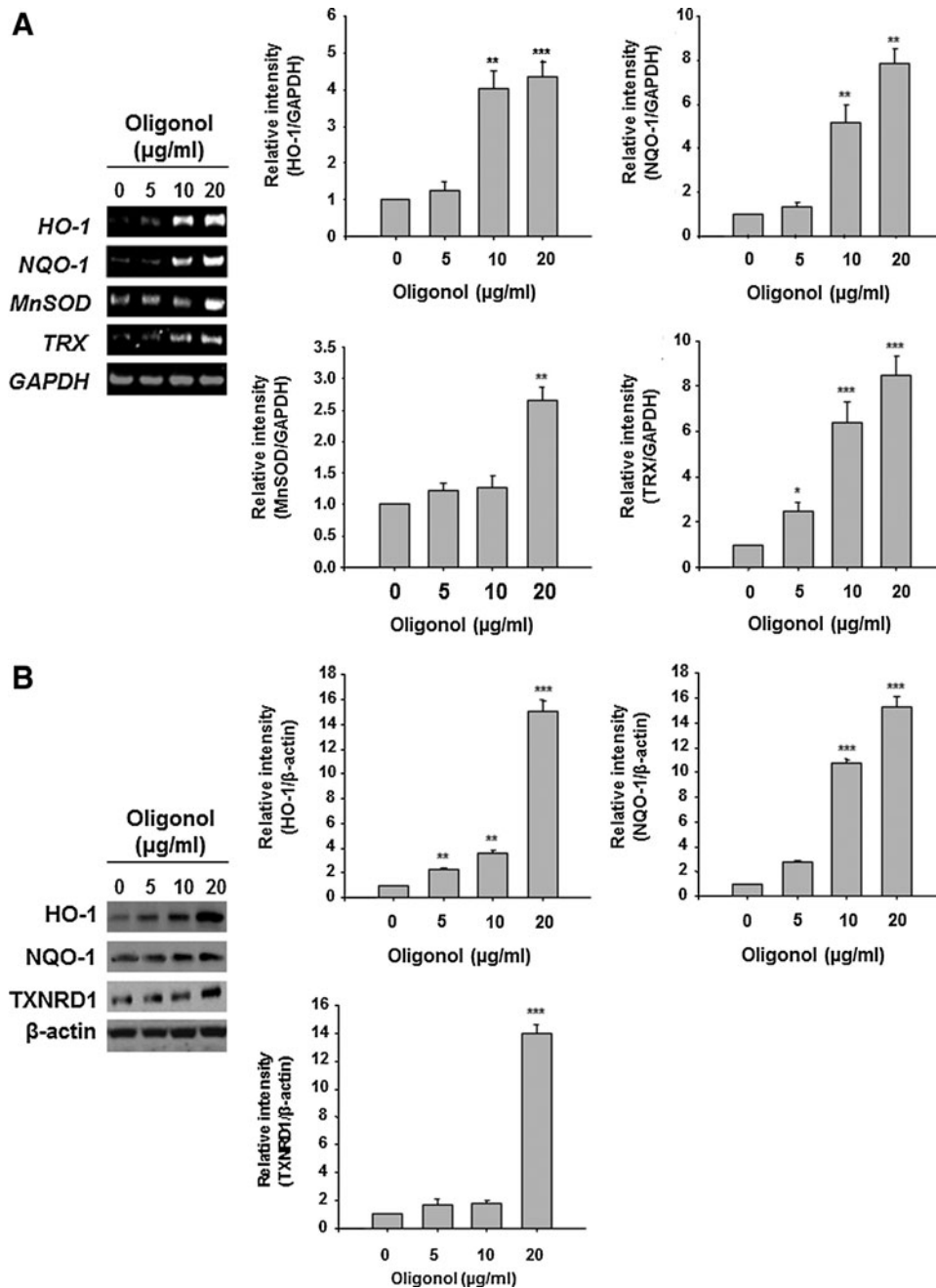

FIG. 7. Oligonol at the indicated concentrations induced the expression of antioxidant enzymes in CCD841CoN cells. (A) RT-PCR analysis of mRNA expression of HO-1, NQO-1, MnSOD, and TRX in CCD841CoN cells. (B) Western blot analysis of HO-1, NQO-1, and TXNRD1 protein expression in CCD841CoN cells. Data represent three independent experiments ($n=3$). Results are expressed as means ± SE. *$p<0.05$, **$p<0.01$, and ***$p<0.001$. TRX, thioredoxin.
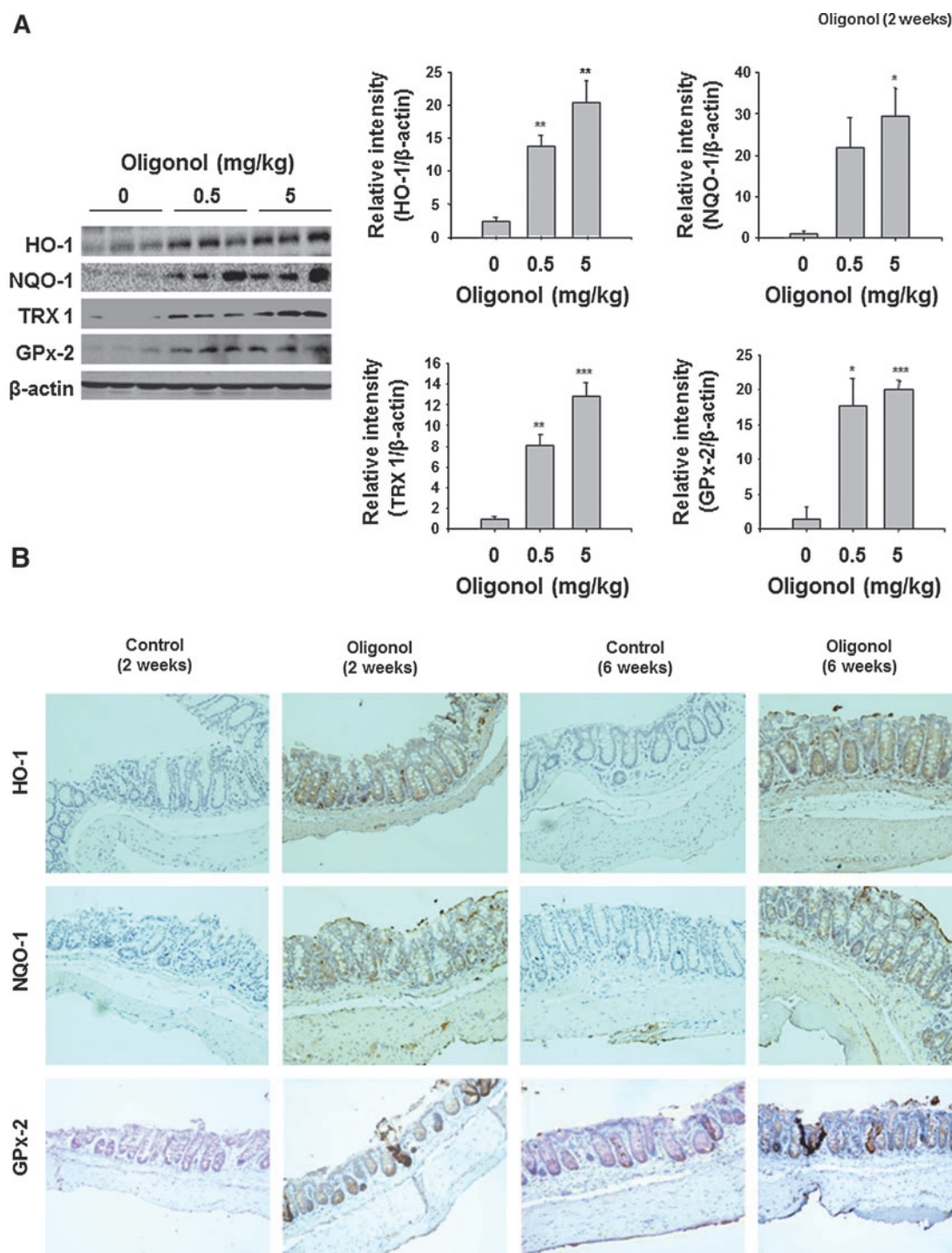
FIG. 8. Oligonol induced the expression of antioxidant enzymes in mouse colon. (A) Western blot analysis of HO-1, NQO-1, TRX 1, and GPx-2 levels in the supernatants of colon strips of control mice and oligonol (0.5 or 5 mg/kg)-treated mice ($n = 5$ each group). Data are expressed as means ± SE. *$p < 0.05$, **$p < 0.01$, and ***$p < 0.001$. **(B)** Immunohistochemical detection of HO-1, NQO-1, and GPx-2 levels (brown spots) in mouse colon. Magnifications × 200. GPx-2, glutathione peroxidase 2.

DSS-promoted two-stage mouse colon tumor model. As depicted in Figure 9A, body weight loss was evident in mice treated with AOM and DSS, and this was less severe in oligonol-treated mice (Fig. 9A). Likewise, the shortening of the colon length caused by AOM plus DSS treatment was attenuated by oligonol administration (Fig. 9B, C). Oral administration of oligonol lowered both the incidence and the multiplicity of colonic adenoma (Table 1). Macroscopically, flat or nodular colonic adenomas were found in the middle and distal colon of the AOM plus DSS group (Fig. 9D). Likewise, histological examination of colon showed that high-grade dysplasia and colonic adenoma were localized in the colonic mucosa of mice treated with AOM and DSS at 8 weeks, all of which were alleviated by oligonol administration (Fig. 9E).
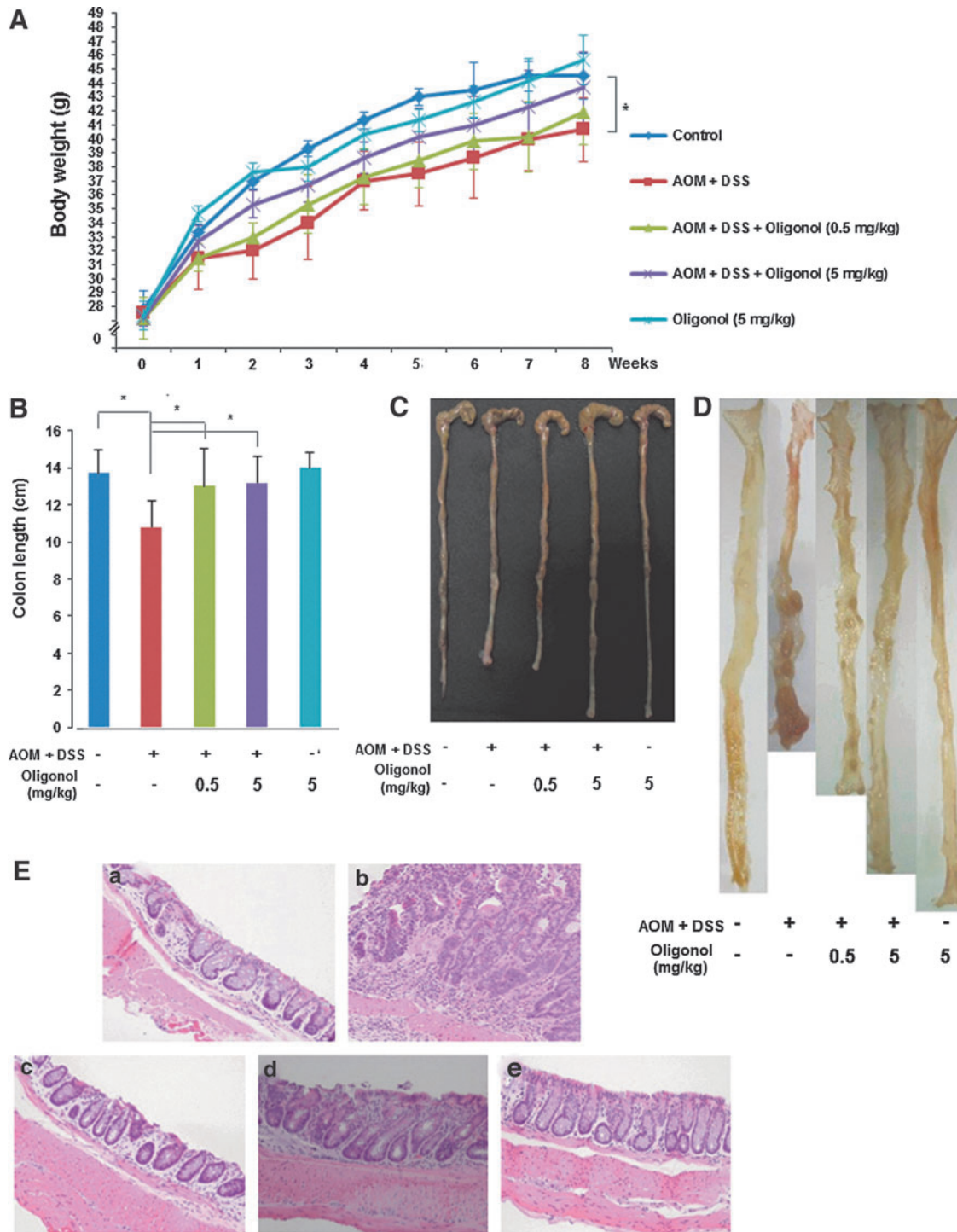
FIG. 9. **Oligonol inhibited AOM plus DSS-induced mouse colon carcinogenesis. (A)** Effects of oligonol on body weight changes in mice treated with AOM+DSS. **(B)** Comparison of the colon length at 8 weeks. Results are expressed as means±SD (n=10 each group). **(C)** A representative photograph of the mouse colon in each group. The incidence and the multiplicity of colonic adenomas. For **(A)** and **(B)**, data are expressed as means±SE (n=10, in each group), *p<0.05. **(D)** Macroscopic view of the mouse colon in each group. **(E)** Histopathology of colonic dysplasia. **(a)** Control; **(b)** AOM+DSS; **(c)** AOM+DSS+Oligonol (0.5 mg/kg); **(d)** AOM+DSS+Oligonol (5 mg/kg); **(e)** Oligonol (5 mg/kg) alone. Animal treatment and other experimental conditions are described in the Materials and Methods section. Magnifications×200.

Discussion

In the present study, we investigated the anti-inflammatory and anticarcinogenic effects of oligonol on the experimental models of colitis and inflammation-associated colon carcino-

genesis. We initially utilized the DSS-induced mouse colitis model that mimics human IBD. Treatment with DSS is known to increase the growth of gram-negative bacteria, which produce LPS and thereby cause colitis *via* the activation of NF-κB and STAT3. Enhanced proliferation of gram-negative

Table 1. Incidence and Multiplicity
of Colonic Adenomas

Treatment group	n	Adenoma incidence (%)	Adenoma multiplicity
Control	10	0.00 (0/10)	0.00
AOM + DSS	10	90.00 (9/10)	7.93 ± 2.02
AOM + DSS + Oligonol (0.5 mg/kg)	10	70.00 (7/10)	4.85 ± 1.19^{a}
AOM + DSS + Oligonol (5 mg/kg)	10	50.00 (5/10)	3.70 ± 1.94^{b}
Oligonol (5 mg/kg)	10	0.00 (0/10)	0.00

Data are expressed as means ± standard error.
[a]$p < 0.05$ and [b]$p < 0.01$ compared with AOM + DSS group.
AOM, azoxymethane; DSS, dextran sulfate sodium.

bacteria in the DSS-treated mouse colon was associated with increased lipid peroxidation (19). Moreover, phagocytes (neutrophils and macrophages) infiltrated into the colonic mucosa are activated by proinflammatory factors that, in turn, stimulate ROS production, particularly superoxide, leading to oxidative stress. Based on these findings, it is speculated that DSS may cause colitis through ROS production and subsequently oxidative tissue damage.

Since the redox-sensitive transcription factors NF-κB and STAT3 regulate proinflammatory gene expression in a cooperative way (10), inhibition of interplay between NF-κB and STAT3 signaling is considered an effective strategy in the management of inflammatory ailments, including IBD. Compelling evidence from population- and laboratory-based studies supports that the inhibition of inappropriate activation of NF-κB and STAT3 by antioxidative and anti-inflammatory substances derived from dietary or medicinal plants are effective for inhibiting IBD. We report here that oligonol abrogates overactivation of NF-κB and STAT3 signaling in colonic mucosa of mice in response to DSS treatment. Another important finding is that oligonol treatment markedly decreased expression of IL-1β, TNF-α, IL-6, COX-2, and iNOS in LPS-stimulated RAW 264.7 cells, and significantly increased the expression of several antioxidant enzymes in the CCD841CoN cells and mouse colonic mucosa. The inhibitory effects of oligonol on expression of proinflammatory cytokines and antioxidant enzymes in cultured cells may account for its anti-inflammatory effect observed in the mouse colon *in vivo*. Considering NF-κB and STAT3 as principal molecular links between inflammation and cancer (26), these findings suggest that oligonol could be a potential candidate in chemoprevention of inflammation-associated colon carcinogenesis. The effect of oligonol on crosstalk between NF-κB and STAT3 signaling, especially with regard to their coordinated roles in suppression of DSS-induced inflammation and carcinogenesis in mouse colon, merits further investigation.

It has been reported that administration of some antioxidants reduces oxidative stress in the experimental colitis models (15). Oligonol administration significantly decreased oxidative stress-induced colonic tissue damage. In the present study, oligonol administration enhanced antioxidant enzyme expression and inhibited DSS-induced apoptosis of epithelial cells in the mouse colon. The intestinal epithelial monolayer could be a target for direct action of oligonol against inflammation as well as oxidative stress. These findings suggest that oral administration of oligonol could preserve the intestinal epithelial barrier through an-

tioxidative and antiapoptotic effects, thus conferring protection against colitis.

Oxidative stress, which often accompanies inflammation, contributes to neoplastic transformation. IBD is considered one of the major oxyradical-overload diseases, whereby chronic inflammation results in a cancer-prone phenotype (14). Kitajima *et al.* demonstrated the presence of macrophages phagocytosing DSS in the middle and distal colon of mice a day after the oral administration of this high-molecular-weight compound, suggesting that DSS could be absorbed in the colonic mucosa and acts as a tumor promoter in the colon carcinogenesis initiated with a low dose of AOM (13). The results from our present study revealed that a single intraperitoneal dose of AOM, followed by 2.5% DSS, produced colonic adenoma at 8 weeks, and oligonol treatment dampened colonic epithelial malignancy induced by AOM plus DSS.

Recently, Fujii *et al.* demonstrated that a serum concentration of total phenolics peaked at 2 h after an oral intake of oligonol (200 mg/day), and a gradual increase in the serum polyphenol content was noted in healthy human subjects receiving oligonol (100 mg/day) for 6 months. According to the acute toxicity study in mice, the LD$_{50}$ of oligonol was found to be 5.024 g/kg body weight, indicative of the relatively safe nature of this formulation. Subacute and chronic toxicity studies in healthy volunteers revealed that the intake of oligonol at doses lower than 200 mg/day did not produce any apparent signs of toxicity (7). We also noticed that treatment of mice with oligonol (5 mg/kg/day) for 6 weeks did not produce any adverse colonic reactions. However, the intestinal absorption and metabolism of oligonol remain largely unknown and need further investigation in the context of the potential application of this formulation in the management of human IBD.

In summary, oligonol provokes antioxidative effects by increasing cytoprotective protein expression, which prevents oxidative stress-induced apoptosis of colonic epithelial cells. In addition, oligonol elicits anti-inflammatory effects by inhibiting DSS-induced activation of NF-κB and STAT3 and their target protein expression and suppresses AOM plus DSS-induced colonic adenoma formation in mice. All these findings, taken together, suggest that this polyphenol formulation has the potential for use to ameliorate IBD and related abnormal conditions, and further clinical studies will be necessary.

Materials and Methods

Animals

Male ICR mice (5 weeks of age) were purchased from Central Lab. Animal, Inc. They were acclimated for 7 days with tap water and a pelleted basal diet before the start of the experiments. The animals were housed in plastic cages under controlled conditions of temperature (23°C ± 2°C), humidity (50% ± 10%), and light (12/12-h light/dark cycle).

Induction of DSS-induced colitis

DSS (molecular weight of 36,000–50,000) was obtained from MP Biomedicals, LLC. Oligonol® (>95% purity) was obtained from Amino Up Chemical Co., Ltd. (Sapporo, Japan). A total of 25 mice were evenly divided into five experimental groups. The mice were treated with 3% DSS in drinking water for 7 days. Oligonol (0.5 or 5 mg/kg/day) was

mixed in tap water and given orally for 7 days before DSS treatment and 7 days together with 3% DSS. After treatment with DSS for 7 days, all mice were sacrificed by cervical dislocation. Their colorectal parts were taken out, cut longitudinally, and washed with phosphate-buffered saline (PBS). For histopathological examination, the distal section of colon tissues was fixed in 10% buffered formalin, whereas another portion was flash-frozen in lipid nitrogen and kept at $-70°C$ for Western blot analysis.

Induction of AOM-initiated and DSS-promoted colon carcinogenesis

AOM was purchased from Sigma Chemical Co. A total of 50 mice were divided into five experimental groups (10 mice per group). The mice received a single intraperitoneal injection of AOM at a dose of 10 mg/kg body weight. Starting 1 week after the AOM injection, animals were exposed to 2.5% DSS in the drinking water for 7 days. Oligonol (0.5 or 5 mg/kg/day) was given orally for 6 weeks after DSS treatment. Mice were then sacrificed by ether overdose at 8 weeks. At autopsy, their large bowel was excised and cut open longitudinally along the main axis. After washing with PBS, the distal section of colon tissues was fixed for histopathological examination.

Histopathological examination

Specimens of the colon fixed with 10% buffered formalin were embedded in paraffin. Each section (4 μm) was stained with H&E. The fixed sections were examined by light microscopy for the presence of lesions. Histological evaluation of the severity of inflammation was performed using a scoring system (4), by a pathologist who was blinded to the treatment.

Immunohistochemical analysis

The dissected colon tissues were prepared for immunohistochemical (IHC) analysis of the expression patterns of MDA, 4-HNE-modified protein, HO-1, NQO-1, and GPx-2. Four-μm sections of 10% formalin-fixed, paraffin-embedded tissues were cut on silanized glass slides and deparaffinized three times with xylene and rehydrated through graded alcohol bath. The deparaffinized sections were heated by using microwave and boiled twice for 6 min in 10 mM citrate buffer (pH 6.0) for antigen retrieval. To diminish nonspecific staining, each section was treated with 3% hydrogen peroxide and 4% peptone casein blocking solution for 15 min. For the detection of respective protein expression, slides were incubated with MDA, 4-HNE (JaICA, Nikken SEIL Co. Ltd.), HO-1 (Stressgen Biotechnologies Co.), NQO-1 (Abcam, Inc.), and GPx-2 (Santa Cruz Biotechnology) antibodies at room temperature for 40 min in Tris-buffered saline containing 0.05% Tween 20, and then developed using respective horseradish peroxidase (HRP)-conjugated secondary antibodies (rabbit, mouse, or goat) EnVision™ System (Dako). The peroxidase-binding sites were detected by staining with 3,3'-diaminobenzidine tetrahydrochloride (Dako). Finally, counterstaining was performed using Mayer's hematoxylin.

TUNEL assay

Apoptosis was detected by the TUNEL assay with the ApopTag® Peroxidase In Situ Apoptosis Detection Kit (Millipore; Cat. S7100). The colon tissues treated with DSS in the presence or absence of oligonol were removed, rinsed with PBS, and fixed in 10% buffered formalin (Fisher) for the TUNEL assay. The apoptotic cells were visualized by light microscopy.

Tissue lysis and protein extraction

Colon tissues were homogenized in an ice-cold lysis buffer (150 mM NaCl, 0.5% Triton-X 100, 50 mM Tris–HCl [pH 7.4], 20 mM ethylene glycol tetra-acetic acid [EGTA], 1 mM dithiothreitol [DTT], 1 mM Na$_3$VO$_4$ and protease inhibitors, 1 mM phenylmethyl sulfonylfluoride [PMSF], and ethylenediaminetetraacetic acid [EDTA]-free cocktail tablet), followed by a periodical vortex for 30 min at 0°C. the lysates were centrifuged at 14,000 rpm for 15 min at 4°C. The supernatants were collected and stored at $-70°C$ until use.

Fractionation of cytosolic and nuclear extracts

Cytosolic extracts were obtained from lysates dissolved in hypotonic buffer A (10 mM 4-(2-hydroxyethyl)-1-piperazineethanesulfonic acid [HEPES] [pH 7.8], 1.5 mM MgCl$_2$, 10 mM KCl, 1 mM DTT, 0.1 mM EDTA, and 0.1 mM PMSF) with 10% Nonidet P-40 (NP-40) by homogenization and vortex mixing at 10-min intervals for 3 h. After centrifugation at 14,000 rpm for 15 min, the supernatants (the cytosolic extracts) were collected and stored at $-70°C$ until use. Precipitated pellets were washed with buffer A plus 10% NP-40 3 times to remove the remaining cytosolic components. Then, the pellets were resuspended in buffer C (50 mM HEPES [pH 7.8], 50 mM KCl, 300 mM NaCl, 0.1 mM EDTA, 1 mM DTT, 0.1 mM PMSF, and 20% glycerol). After centrifugation at 14,000 rpm for 15 min, the supernatants (nuclear extracts) were collected and stored at $-70°C$ until use.

Western blot analysis

For Western blot analysis, the total protein concentration was quantified by using the bichinconinic acid (BCA) protein assay kit (Pierce). Cell lysates (30–50 μg protein) were mixed and boiled in a sodium dodecyl sulfate (SDS) sample buffer for 5 min before 8%–15% SDS–polyacrylamide gel electrophoresis (SDS-PAGE). They were separated by SDS-PAGE and transferred to a polyvinylidene difluoride (PVDF) membrane (Gelman Laboratory). The blots were blocked in 5% fat-free dry milk in Tris-buffered saline containing 0.1% Tween 20 (TBST) for 1 h at room temperature. The membranes were incubated for 12–24 h at 4°C with dilutions of primary antibodies for α-tubulin, IκBα, p-p65, GPx-2 (Santa Cruz Biotechnology), lamin-B (Invitrogen), actin (Sigma Aldrich), p-IκBα, p65, p-STAT3, STAT3, cyclin D1, TXN 1 (Cell Signaling Technology), COX-2 (Cayman Chemical), iNOS (BD Biosciences), HO-1 (Stressgen Biotechnologies Co.), NQO-1, and TXNRD1 (Abcam, Inc.). The membranes were washed, followed by incubation with 1:4000 dilution of respective HRP-conjugated secondary antibodies (rabbit, mouse or goat) (Zymed Laboratories) for 2 h, and again washed with TBST. Protein expressed was visualized with an enhanced chemiluminescence detection kit (Amersham Pharmacia Biotech) and LAS-4000 image reader (Fugi film) according to the manufacturer's instructions.

Cell culture

The RAW 264.7 cells were obtained from the American Type Culture Collection and maintained in DMEM containing 10%

fetal bovine serum (FBS) and an antibiotic–antimycotic mixture (Gibco BRL) at 37°C with 5% CO_2 and 95% air. The RAW 264.7 cells were treated with LPS (200 ng/ml; Sigma Aldrich) in the presence or absence of oligonol (10 or 20 μg/ml).

The CCD841CoN cells were obtained from the American Type Culture Collection and maintained in an MEM containing 10% FBS and ajn antibiotic–antimycotic mixture (Gibco BRL). CCD841CoN cells were treated with oligonol (5, 10, or 20 μg/ml) for 3–24 h.

After treatment, the media in the apical side were harvested and centrifuged at 7500 g for 5 min at 4°C. The cells were suspended in the cell lysis buffer (Cell Signaling Technology). After centrifugation at 13,000 g for 15 min, the supernatant was collected and stored at -70°C until use.

Reverse transcription–polymerase chain reaction analysis

Total RNA was isolated from RAW 264.7 and CCD841CoN cells using TRIzol® reagent (Invitrogen) according to the manufacturer's protocol. To generate the cDNA from RNA, 1 μg of total RNA was reverse transcribed with murine leukemia virus reverse transcriptase (Promega) for 50 min at 42°C and again for 15 min at 72°C. About 1 μl of cDNA was amplified with a PCR mixture (HyMed) in sequential reactions. The primers used for each reverse transcription–polymerase chain reaction reactions are as follows: *IL-1β*, 5′-GCC CAT CCT CTG TGA CTC AT-3′and 5′-AGG CCA CAG GTA TTT TGT CG-3′; *TNF-α*, 5′-TGA ACT TCG GGG TGA TCG GTC-3′ and 5′-AGC CTT GTC CCT TGA AGA GAA C-3′; *IL-6*, 5′-AGT TGC CTT CTT GGG ACT GA-3′ and 5′-TCC ACG ATT TCC CAG AGA AC-3′; *COX-2*, 5′-CTG GTG CCT GGT CTG ATG ATG-3′ and 5′-GGC AAT GCG GTT CTG ATA CTG-3′; *iNOS*, 5′-GTT CTC AGC CCA ACA ATA CAA GA-3′ and 5′-GTG GAC GGG TCG ATG TCA C-3′; *Actin*, 5′-AGA GCA TAG CCC TCG TAG AT-3′ and 5′-CCC AGA GCA AGA GAG GTA TC-3′; *HO-1*, 5′-CAG GCA GAG AAT GCT GAG TTC-3′and 5′-GAT GTT GAG CAG GAA CGC T-3′; *NQO-1*, 5′-GAG GAC CTC CTT CAA CTA TG-3′ and 5′-CCT TTG TCA TAC ATG GCA GC-3′; *MnSOD*, 5′-CCT GAA CGT CAC CGA GGA GAA G-3′ and 5′-CTC CCA GTT GAT TAC ATT AGT-3′; *TRX*, 5′- GCT CAG GAG GTC TGG CAG CTG CTA AG-3′ and 5′-GTG CAA GCA TCT CTT CCT ATT GCC AG-3′; *GAPDH*, 5′-AAG GTC GGA GTC AAC GGA TTT-3′ and 5′-GCA GTG AGG GTC TCT CT-3′ (forward and reverse, respectively). Amplification products were analyzed by 2% agarose gel electrophoresis, followed by staining with SYBR Green (Invitrogen) and photographed using fluorescence in LAS-4000 (Fugi film).

Statistical analysis

Except for the data on the DAI score, colon length, and histologic inflammatory score expressed as the mean±standard deviation, all the other values were expressed as the mean±standard error of at least three independent experiments. Statistical significance was determined by the Student's t-test, and $p < 0.05$ was considered to be statistically significant.

Acknowledgments

Author Disclosure Statement

No competing financial interest exists.

References

1. Artis D. Epithelial-cell recognition of commensal bacteria and maintenance of immune homeostasis in the gut. *Nat Rev Immunol* 8: 411–420, 2008.
2. Buettner R, Mora LB, and Jove R. Activated STAT signaling in human tumors provides novel molecular targets for therapeutic intervention. *Clin Cancer Res* 8: 945–954, 2002.
3. Buffinton GD and Doe WF. Depleted mucosal antioxidant defences in inflammatory bowel disease. *Free Radic Biol Med* 19: 911–918, 1995.
4. Cheon JH, Kim JS, Kim JM, Kim N, Jung HC, and Song IS. Plant sterol guggulsterone inhibits nuclear factor-kappaB signaling in intestinal epithelial cells by blocking IkappaB kinase and ameliorates acute murine colitis. *Inflamm Bowel Dis* 12: 1152–1161, 2006.
5. Elson CO, Sartor RB, Tennyson GS, and Riddell RH. Experimental models of inflammatory bowel disease. *Gastroenterology* 109: 1344–1367, 1995.
6. Fresco P, Borges F, Diniz C, and Marques MP. New insights on the anticancer properties of dietary polyphenols. *Med Res Rev* 26: 747–766, 2006.
7. Fujii H, Sun B, Nishioka H, Hirose A, and Aruoma OI. Evaluation of the safety and toxicity of the oligomerized polyphenol Oligonol. *Food Chem Toxicol* 45: 378–387, 2007.
8. Fujii H, Yokozawa T, Kim YA, Tohda C, and Nonaka G. Protective effect of grape seed polyphenols against high glucose-induced oxidative stress. *Biosci Biotechnol Biochem* 70: 2104–2111, 2006.
9. Ghosh S and Hayden MS. New regulators of NF-kappaB in inflammation. *Nat Rev Immunol* 8: 837–848, 2008.
10. Grivennikov SI and Karin M. Dangerous liaisons: STAT3 and NF-kappaB collaboration and crosstalk in cancer. *Cytokine Growth Factor Rev* 21: 11–19, 2010.
11. Jo EH, Lee SJ, Ahn NS, Park JS, Hwang JW, Kim SH, Aruoma OI, Lee YS, and Kang KS. Induction of apoptosis in MCF-7 and MDA-MB-231 breast cancer cells by Oligonol is mediated by Bcl-2 family regulation and MEK/ERK signaling. *Eur J Cancer Prev* 16: 342–347, 2007.
12. Keklikoglu N, Koray M, Kocaelli H, and Akinci S. iNOS expression in oral and gastrointestinal tract mucosa. *Dig Dis Sci* 53: 1437–1442, 2008.
13. Kitajima S, Takuma S, and Morimoto M. Tissue distribution of dextran sulfate sodium (DSS) in the acute phase of murine DSS-induced colitis. *J Vet Med Sci* 61: 67–70, 1999.
14. Klaunig JE and Kamendulis LM. The role of oxidative stress in carcinogenesis. *Annu Rev Pharmacol Toxicol* 44: 239–267, 2004.
15. Krieglstein CF, Cerwinka WH, Laroux FS, Salter JW, Russell JM, Schuermann G, Grisham MB, Ross CR, and Granger DN. Regulation of murine intestinal inflammation by reactive metabolites of oxygen and nitrogen: divergent roles of superoxide and nitric oxide. *J Exp Med* 194: 1207–1218, 2001.
16. Kundu JK, Chang EJ, Fujii H, Sun B, and Surh YJ. Oligonol inhibits UVB-induced COX-2 expression in HR-1 hairless mouse skin—AP-1 and C/EBP as potential upstream targets. *Photochem Photobiol* 84: 399–406, 2008.

17. Kundu JK, Hwang DM, Lee JC, Chang EJ, Shin YK, Fujii H, Sun B, and Surh YJ. Inhibitory effects of oligonol on phorbol ester-induced tumor promotion and COX-2 expression in mouse skin: NF-kappaB and C/EBP as potential targets. *Cancer Lett* 273: 86–97, 2009.

18. Lavi I, Levinson D, Peri I, Nimri L, Hadar Y, and Schwartz B. Orally administered glucans from the edible mushroom Pleurotus pulmonarius reduce acute inflammation in dextran sulfate sodium-induced experimental colitis. *Br J Nutr* 103: 393–402, 2010.

19. Lee IA, Bae EA, Hyun YJ, and Kim DH. Dextran sulfate sodium and 2,4,6-trinitrobenzene sulfonic acid induce lipid peroxidation by the proliferation of intestinal gram-negative bacteria in mice. *J Inflamm (Lond)* 7: 7, 2010.

20. Maloy KJ and Powrie F. Intestinal homeostasis and its breakdown in inflammatory bowel disease. *Nature* 474: 298–306, 2011.

21. Perkins ND. Post-translational modifications regulating the activity and function of the nuclear factor kappa B pathway. *Oncogene* 25: 6717–6730, 2006.

22. Saleh M and Trinchieri G. Innate immune mechanisms of colitis and colitis-associated colorectal cancer. *Nat Rev Immunol* 11: 9–20, 2011.

23. Shapiro H, Singer P, Halpern Z, and Bruck R. Polyphenols in the treatment of inflammatory bowel disease and acute pancreatitis. *Gut* 56: 426–435, 2007.

24. Tanaka T, Kohno H, Suzuki R, Yamada Y, Sugie S, and Mori H. A novel inflammation-related mouse colon carcinogenesis model induced by azoxymethane and dextran sodium sulfate. *Cancer Sci* 94: 965–973, 2003.

25. Tanaka T, Kohno H, Yoshitani S, Takashima S, Okumura A, Murakami A, and Hosokawa M. Ligands for peroxisome proliferator-activated receptors alpha and gamma inhibit chemically induced colitis and formation of aberrant crypt foci in rats. *Cancer Res* 61: 2424–2428, 2001.

26. Terzic J, Grivennikov S, Karin E, and Karin M. Inflammation and colon cancer. *Gastroenterology* 138: 2101–2114.e5, 2010.

Address correspondence to:
Prof. Young-Joon Surh
Tumor Microenvironment Global Core Research Center
College of Pharmacy
Seoul National University
599 Gwanak-ro
Gwank-gu
Seoul 151-742
South Korea

E-mail: surh@plaza.snu.ac.kr

Abbreviations Used

4-HNE = 4-hydroxy-2-nonenal
AOM = azoxymethane
AP-1 = activator protein-1
BCA = bichinconinic acid
C/EBP = CCAAT/enhancer-binding protein
COX-2 = cyclooxygenase-2
CRC = colorectal cancer
DAI = disease activity index
DSS = dextran sulfate sodium
DTT = dithiothreitol
EDTA = ethylenediaminetetraacetic acid
EGTA = ethylene glycol tetra-acetic acid
ERK = extracellular signal-regulated protein kinase
FBS = fetal bovine serum
GPx-2 = glutathione peroxidase 2
H&E = hematoxylin and eosin
HEPES = 4-(2-hydroxyethyl)-1-piperazineethanesulfonic acid
HO-1 = heme oxygenase-1
HRP = horseradish peroxidase
IBD = inflammatory bowel disease
IHC = immunohistochemical
IL = interleukin
iNOS = inducible nitric oxide synthase
IκB = inhibitor of κB
KO = knockout
LPS = lipopolysaccharide
MAP = mitogen-activated protein
MDA = malondialdehyde
MnSOD = manganese superoxide dismutase
NF-κB = nuclear factor-kappa B
NP-40 = Nonidet P-40
NQO-1 = NAD(P)H:quinone oxidoreductase 1
PAGE = polyacrylamide gel electrophoresis
PBS = phosphate-buffered saline
PMSF = phenylmethyl sulfonylfluoride
PVDF = polyvinylidene difluoride
ROS = reactive oxygen species
RT-PCR = reverse transcription–polymerase chain reaction
SD = standard deviation
SDS = sodium dodecyl sulfate
SE = standard error
STAT = signal transducer and activator of transcription
TAD = transactivation domain
TBST = Tris-buffered saline containing 0.1% Tween 20
TLR = Toll-like receptor
TNBS = trinitrobenzene sulfonic acid
TNF = tumor necrosis factor
TPA = 12-*O*-tetradecanoylphorbol-13-acetate
TUNEL = terminal deoxynucleotidyl transferase dUTP nick-end labeling
TRX = thioredoxin
TXNRD1 = thioredoxin reductase 1
WT = wild-type